Influence of Time on Crystal Attrition in a Stirred Vessel

B. Mazzarotta, S. Di Cave, and G. Bonifazi
Dept. of Chemical Engineering, University of Rome "La Sapienza," I-00184, Rome, Italy

Attrition is the unwanted breakdown of particles within a process, mainly as a consequence of collisions with other particles or parts of the equipment. The relevant mechanisms are abrasion, defined as the removal of material much smaller than the particle, and shatter (or fragmentation or breakage), defined as the splitting of a particle into smaller parts (Bemrose and Bridgwater, 1987). Abrasion requires lower impact energy (Kelly and Spottiswood, 1982), and is recognized to prevail in crystal suspensions (see, for example, Nienow and Conti, 1978; Conti and Nienow, 1980; and Mazzarotta, 1992).

A useful perspective on crystal attrition is found in the works of Fasoli and Conti (1973), Chianese et al. (1986), Ayazi Shamlou et al. (1990), Synowiec et al. (1993), and Gahn and Mersmann (1995). However, no generally accepted method for quantifying attrition has been assessed, although a number of attrition rates have been defined, such as the number of abrasion fragments produced per abrading particle (Fasoli and Conti, 1973; Nienow and Conti, 1978; Synowiec et al., 1993), the mass-abrasion rate of the fragments (Chianese et al., 1986), and the initial rate of fragment generation (Ayazi-Shamlou et al., 1990).

In fact, crystal attrition does not simply generate large amounts of small fragments, but affects the size distribution and the morphology of all the crystals. The breakage functions commonly adopted to describe the product of comminution events (Kelly and Spottiswood, 1982) give unsatisfactory results when applied to crystal attrition, since abrasion fracture, which originates a bimodal size distribution, predominates. Encouraging results were obtained using a model combining abrasion and shatter fracture (Mazzarotta, 1992, 1993), although the number of parameters increased.

On the other hand, the information concerning the morphology of the product of crystal attrition appears limited to qualitative remarks about photographs of the large abraded crystals and of the fine fragments (Fasoli and Conti, 1973; Conti and Nienow, 1980).

The objective of the present work is to investigate the effect of time on crystal attrition by carefully examining how the size distribution and the morphology of the fragments, generated by attrition of large regular crystals, evolve with time.

Experimental Technique

The sieve fraction 1.18–1.4 mm of regularly shaped commercial sugar crystals was used for the experiments. The crystals were dispersed into a mixture of xylenes, nonsolvent for sugar, in order to avoid any crystallization or dissolution phenomena during the run.

The experimental vessel was cylindrical (ID, 140 mm; height, 350 mm) with a conical bottom (height, 150 mm) and four radial baffles, 15 mm wide, which follow the vessel profile, allowing 1 mm clearance from the walls. Stirring was supplied by a 70 mm marine propeller, rotating 85 mm above the apex of the cone and the rotating speed was set at 18.33 RPS, based upon the criterion that no crystal remained on the bottom for longer than 1–2 s.

The density of the suspension was 100 kg/m^3, which corresponds to a reasonable value for a crystallizer, obtained by mixing 300 g of crystals and 3 L of xylene. After stirring for the required period of time, the suspension was discharged and filtered under a vacuum using a Whatman N.3 filter. The experiments were carried out at ambient temperature (18–22°C). No appreciable temperature buildup occurred during the runs.

The recovered crystals were dried in the hood at ambient temperature for one day and then sieved, using ASTM sieves, 100 mm in diameter, down to 0.3 mm. The fractions, obtained after 20 min of shaking, were placed into separated air tight bags. Preliminary tests showed that sieving did not produce any appreciable change in the size distribution. The amount of product lost during discharge, filtering and sieving operations was less than 0.5%.

The size distribution of the material below 0.3 mm was determined, down to 5.8 μm, using a laser light diffraction granulometer (Malvern 3600). The measurements were taken under agitation at 3–5 min intervals, until a good reproducibility was achieved: this required up to 1 h for agglomerated fragments. However, due to the very low suspension density (< 0.02 vol. %), such prolonged stirring did not ap-

Correspondence concerning this article should be addressed to B. Mazzarotta.

Table 1. Operating Conditions of Attrition Runs and Values of the Parameters of the Model Interpolated as Functions of the Time

Run	Time (min)	L_f (μm)	L_c (mm)	y_{fines}	k_s	n_s
1	1	14.1	0.776	0.00012	0.0019	0.974
2	5	17.2	0.823	0.00018	0.0027	0.711
3	10	18.7	0.870	0.00064	0.0037	0.597
4	20	20.3	0.935	0.00284	0.0060	0.484
5	30	21.3	0.973	0.00614	0.0088	0.417
6	45	22.4	1.005	0.0121	0.0144	0.351
7	60	23.2	1.020	0.0185	0.0223	0.304
8	90	24.3	1.030	0.0316	0.0063	1.5
9	120	25.2	1.032	0.0442	0.0063	1.5
10	180	26.5	1.033	0.0673	0.0063	1.5
11	240	27.4	1.033	0.0875	0.0063	1.5
12	360	28.8	1.033	0.121	0.0063	1.5
13	480	30.6	1.033	0.149	0.0063	1.5

preciably modify the original size distribution. The morphology of the original crystals and sieve fractions obtained from each run was studied by image analysis. Particle images, containing 4–18 fragments, were acquired using a Leica Wild M2 stereomicroscope connected to a video camera (I2S IEC 800 CC) and were digitized using a frame grabber (Matrox MPV AT) on a personal computer. Four images were taken from each sieve fraction to achieve statistical significance.

Results

A total of 13 attrition experiments, ranging from 1 min to 8 h, were carried out, Table 1. Three of the runs were duplicated: the reproducibility was good, both in terms of size distribution and of morphological parameters.

The overall amount of fragments (i.e., of particles falling below the original size range), $y_{fragments}$, is plotted vs. time t in Figure 1. The crystals undergo copious and almost instantaneous attrition as soon as stirring starts: after 1 min the fragments are more than 19%. This quantity remains practically constant during the subsequent 10 min; then increases, first rapidly (34% after 1 h), then more slowly (60% after 8 h).

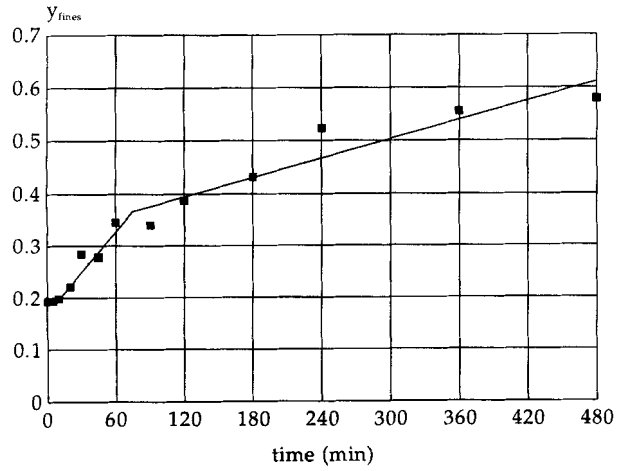

Figure 1. Overall mass of the fragments vs. time.

Symbols = experimental data; lines = curves calculated using the values of the attrition rate listed in Table 2.

An average fragment generation rate R_f defined as mass of fragments generated per unit time and unit volume, was calculated for each of the above time intervals, fitting the data by means of straight lines. A fair agreement was obtained, as shown in Figure 1: the value of R_f, listed in Table 2, reduces by a factor 4, after the first 1 h of stirring.

The size distributions of the fragments are shown in Figure 2, as a cumulative mass fraction y_{wt} vs. size L in log-log graphs: to improve clarity only six runs are presented. Such cumulative plots are commonly used to show the results of comminution processes (Kelly and Spottiswood, 1982). The logarithmic coordinates enlarge the zone of the small fragments, but do not allow direct comparison of the slopes.

All the curves show similar trends: proceeding from large to small sizes, the slope is first sharp, down to about 0.6 mm, then declines in the central part, and finally increases in its last portion, roughly below 0.01 mm. These trends are typical of bimodal distributions, with a main peak in the coarse fragments region, and a much lower peak in the fine fragments one. Figure 2 shows the curves regularly moving toward higher y_{wt} values as the time proceeds, which means an increment in the amount of generated fragments.

The morphology of a particle can be described using a number of shape parameters, such as roundness, surface and volume shape factors, elongation ratio, and so on. The roundness

$$\Phi = \frac{\text{perimeter}^2}{4\pi\,\text{area}} \tag{1}$$

was selected as the characteristic morphological parameter since it uses all the points on the boundary of the surface of

Table 2. Rates of Fragment Generation

Time Interval	Rate of Fragment Generation (kg/m^3·h)
0 min–1 min	1,154
1 min–10 min	2.7
10 min–60 min	15.7
90 min–8 h	3.7

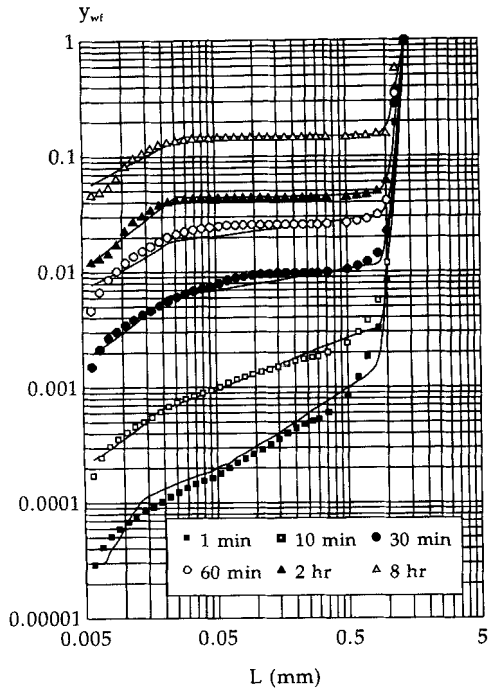

Figure 2. Size distribution of the product obtained from the attrition runs.

Symbols = experimental data; lines = curves calculated introducing in the model the values of the parameters listed in Table 1.

the particle profile, thus retaining the highest information content (Beddow, 1984). The values of the roundness are generally greater than unity (roundness of a sphere), and approach this value as the particle becomes more spherical.

The roundness of the initial crystals was equal to 1.28 with standard deviation 0.04, which is an index of a regular shape as well as of a good morphological similarity.

The trend of the roundness vs. time, is shown in Figure 3 for four typical classes of fragments ranging from the crystals still falling in the original size range to small fragments (0.3–0.355 mm). The roundness of each examined fraction

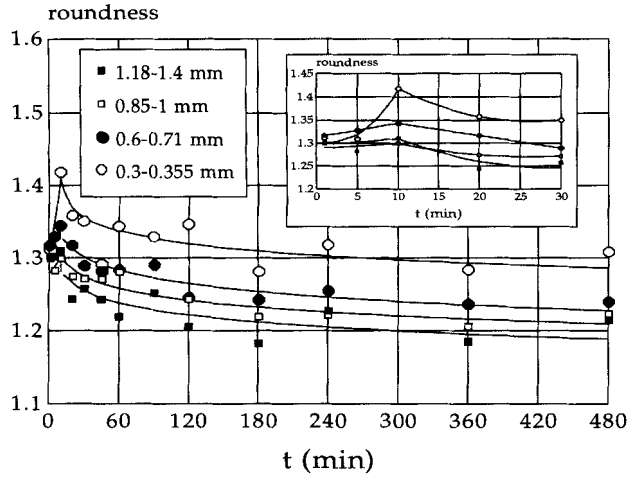

Figure 3. Roundness of selected size fractions of fragments vs. time.

increases during the first 10 min, then gradually declines toward an almost constant value. At any fixed time, the values of the roundness increases by decreasing the fragment size, indicating a less spherical shape.

Modeling

The crystal attrition model proposed by Mazzarotta (1992) was used. It makes use of the following assumptions: 1) abrasion generates only fragments below L_f, the maximum size of the fine fragments, and leaves a coarse residue larger than L_c, minimum size of the coarse residue; 2) shatter generates fragments of all sizes; 3) the cumulative mass fraction of the attrition fragments, y_{wt}, can be obtained by linearly combining the size distributions of the fragments generated by abrasion and shatter (Stanley, 1974)

$$y_{wt} = k_s y_{ws} + (1 - k_s)(y_{wf} + y_{wc}) \tag{2}$$

where k_s is the contribution of shatter to attrition, and $(1 - k_s)$ is that of abrasion; 4) the cumulative mass fractions of the fragments can be estimated using the expression (Broadbent and Callcott, 1956)

$$y_w = \frac{1 - \exp\left[-\left(\frac{L}{L_{\max}}\right)^n\right]}{1 - \exp(-1)} \tag{3}$$

where $L_{\max}$ is the maximum size of the initial crystals, y_w is the cumulative mass fraction, and n the distribution modulus, which assume the values y_{wf}, n_f, and y_{wc}, n_c for the fine and coarse abrasion fragments, respectively, and y_{ws}, n_s for the shatter fragments.

The model is completed by the equation expressing the congruity conditions (abrasion does not generate fragments in the size range $L_f - L_c$)

$$y_{wf}(L_f) = y_{wc}(L_c) \tag{4}$$

and by defining the overall mass fraction of fine fragments, y_{fines}, of size below L_f

$$y_{\text{fines}} = k_s y_{ws}(L_f) + (1 - k_s) y_{wf}(L_f) \tag{5}$$

Therefore, the model contains 5 independent parameters, which are L_f, L_c, n_s, k_s and y_{fines}. The attrition model was applied to fit the experimental size distributions, by using a regression procedure (Rosenbrock and Storey, 1966) which minimizes the percentage differences between calculated and experimental values to adequately weight the contribution of the fine fragments. The fitting was excellent for all the runs.

The trend of the parameters of the model vs. time is shown in Figure 4. The values of L_f and L_c increase with increasing time, in the ranges 11–30 μm and 0.75–1 mm, respectively: they correspond reasonably to the abscissae at which the slopes of the curves y_{wf} vs. t change (see Figure 2). Also y_{fines} increases from 0.01 wt. % after 1 min to 15 wt. % after 8 h: taking into account the trend of the overall fragment

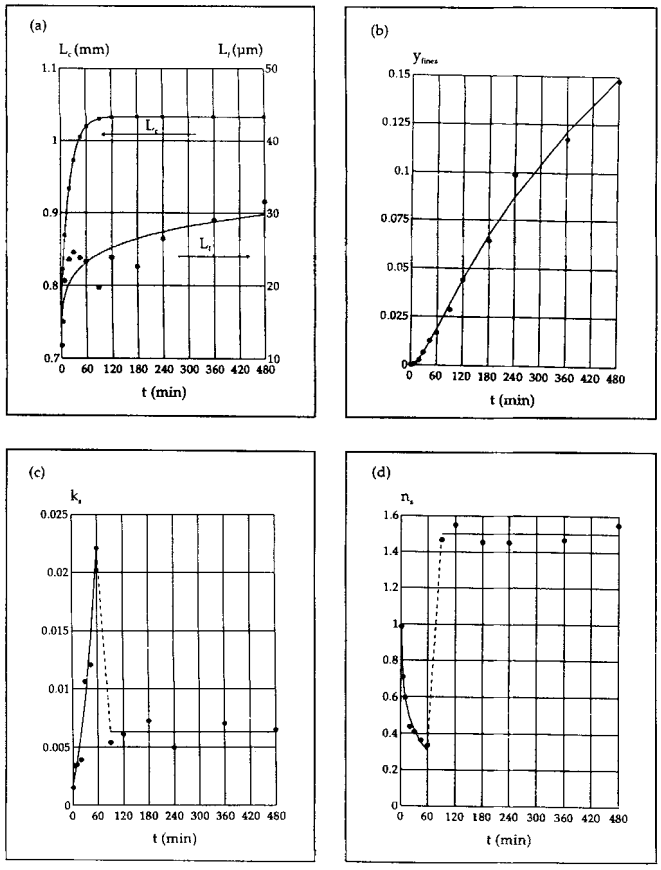

Figure 4. Parameters of the attrition model vs. time.

Symbols = values calculated applying the regression procedure to fit the size distributions; lines = values interpolated using the expressions listed in Table 3.

production (see Figure 1) this means that the proportion of small fragments increases as attrition proceeds.

The trends of the parameters related to shatter fracture, k_s and n_s, appear specular and exhibit a discontinuity after 1 h. The low values of k_s confirm a minor contribution of shatter to attrition: however, they increase in the first 1 h up to more than 2%, then slow down fluctuating around 0.6%. Correspondingly, n_s decreases from 0.9 to 0.3 in the first 60 min, then rises to a constant value around 1.5. The average size of the shatter fragments, calculated by Eq. 3 to be 0.5 mm after 1 min, progressively reduces to 0.055 mm after 1 h, then fluctuates around 0.7 mm until the end of the run. Therefore, in the initial phase the contribution of shatter to attrition increases and the crystals are broken into progressively smaller pieces; subsequently, its importance reduces and the crystals are split into much larger fragments. The values of the parameters were fitted using the empirical expressions listed in Table 3, obtaining a reasonable agreement, as shown in Figure 4. The values of the parameters calculated from this fitting (listed in Table 1) were inserted into the model, and the corresponding size distributions were calculated. They compared acceptably with the experimental data, as shown in Figure 2.

Table 3. Expressions of Parameters of the Model as Functions of Time

$L_f = 0.0141t^{0.121}$ (in mm)	(1 min $< t <$ 8 h)
$L_c = 0.270\,[3.829 - \exp(-0.0503t)]$ (in mm)	(1 min $< t <$ 8 h)
$y_{\text{fines}} = 0.00012\,\exp(-17.17t^{-0.356})$	(1 min $< t <$ 8 h)
$k_s = \exp(-6.504 + 0.223t^{0.609})$	(1 min $< t <$ 1 h)
$k_s = 0.00632$	(1.5 h $< t <$ 8 h)
$n_s = 0.974 - 0.164 \ln t$	(1 min $< t <$ 1 h)
$n_s = 1.5$	(1.5 h $< t <$ 8 h)

Discussion

The results showed that the influence of time on crystal attrition was remarkable, and affected the amount of generated fragments, their size distribution and their morphology.

With reference to Figure 1, the overall fragment generation appears massive in the first min, negligible from 1 to 10 min, high from 10 min to 1 h and moderate from 1 to 8 h.

Usually, most of the nuclei production occurring as crystals are suspended in a liquid. This is ascribed to "initial breeding" and "needle breeding" mechanisms (Strickland-Constable, 1968). The first consists of detachment of crystalline dust from the surface of the crystals, and the latter the removal of dendrites. Both are expected to generate tiny fragments. In the present case, based on the habit of the crystals, needle breeding is not likely to occur, while some initial breeding may derive from the sieving of the used crystals. However, the size distribution of the crystals after 1-min stirring (19.3% of fragments, but just 0.1% below 0.5 mm) is similar to those determined in other cases of crystal attrition (Fasoli and Conti, 1973; Mazzarotta, 1992) suggesting that relatively large pieces were detached from the original crystals. Moreover, the roundness of the crystals surviving in the original size range grows from 1.28 to 1.30 in the first min, and slightly increases to 1.31 in the first 10 min. This means that the crystals become less spherical, as though a not negligible fracture occurred.

All this considered, the hypothesis can be made that the strong initial attrition depends on the presence of microscopic cracks or flaws in the structure of the used crystals. In these points the strength of the crystals is reduced and the fracture can occur on impact, also at relatively low collision energy. Such a mechanism can explain both the considerable amount of fragments generated in the first instance and the rapid decline of this phenomenon in the minutes immediately following.

After the initial period, the roundness of the fragments decreases regularly (see Figure 3), i.e., they become more spherical as attrition proceeds, in agreement with the findings of other researchers (Fasoli and Conti, 1973; Nienow and Conti, 1978) who took photographs of abraded crystals after stirring for some hours. A progressive reduction of the attrition rate is also expected based on the size reduction of the largest crystals (> 1 mm), whose collisions are the most energetic, from the initial value of 1.29 to the final one of 1.19. However, this corresponds to a decrease of about 21% of the kinetic energy, and therefore, cannot explain the remarkable reduction of the fragment generation rate R_f after 1 h. On the other hand, the trends of the parameter n_s and k_s show that in the first 1 h increasing amounts of progressively smaller shatter fragments are generated, while, subsequently, their quantity is lower and their size much larger, although the frequency of the most energetic impacts capable of crushing the crystals does not change during the run.

The hypothesis can be made that, in the first 1 h, the crystals presenting defects become progressively fractured into small pieces. The surviving crystals are more resistant, probably also due to their more spherical shape, but suffer from several repeated low-energy collisions, which may induce "fatigue" stress, causing a drastic reduction of their strength after a number of cycles. Crystals suffering this type of stress, which requires a lengthy period of stirring before developing, may be split into pieces on receiving moderate impacts.

Conclusion

The effect of time on crystal attrition is remarkable. First, a transitory phase (about 10 min) occurs. In the first minute a great amount of fragments are generated but immediately afterwards the fragment production becomes negligible. This behavior is likely to depend on cracks initially present in the crystals with the detachment of such pieces from the crystals causing their shape to become less rounded. Subsequently, the fragments become progressively more rounded as time proceeds, while the fragment generation rate is relatively high and almost constant up to 1 h before decreasing significantly. The use of a crystal attrition model to fit the data confirmed the large predominance of abrasion over shatter fracture. In particular, during the first 1 h, the contribution of shatter increases up to 2%, generating progressively smaller fragments. This mechanism is likely to crush the majority of the crystals presenting defects. In fact, after 1 h, the attrition rate decreases, probably since the residual crystals, which present fewer defects, are more resistant. In this final period (1–8 h) shatter reduces its influence to 0.6% and generates large fragments: this may be due to some "fatigue" fracture, possibly due to repeated low-energy-impacts, which are able to split the crystals into relatively big pieces.

Acknowledgment

The authors gratefully acknowledge the contribution of Mr. M. Alfano and Mr. E. De Paola to the experimental work and are thankful for the financial support of MURST, Italy.

Literature Cited

Ayazi-Shamlou, P., A. G. Jones, and K. Djamarani, "Hydrodynamics of Secondary Nucleation in Suspension Crystallization," *Chem. Eng. Sci.*, **45,** 1405 (1990).

Beddow, J. K., "Recent Applications of Morphological Analysis," *Particle Characterization in Technology: II. Morphological Analysis*, J. K. Beddow, ed., CRC Press, Boca Raton, FL, p. 149 (1984).

Bemrose, C. R., and J. Bridgwater, "A Review of Attrition and Attrition Test Methods," *Powder Tech.*, **49,** 97 (1987).

Broadbent, S. R., and T. G. Callcott, "Coal Breakage Processes," *J. Inst. Fuel*, **29,** 524 (1956).

Chianese, A., S. Di Cave, and B. Mazzarotta, "Secondary Nucleation by Abrasion of Potassium Sulphate," *Proc. World Cong. of Chem. Eng.*, Vol. II, Tokyo, p. 937 (Sept. 21–25, 1986).

Conti, R., and A. W. Nienow, "Particle Abrasion at High Solids Concentration in Stirred Vessels—II," *Chem. Eng. Sci.*, **35,** 543 (1980).

Fasoli, U., and R. Conti, "Crystal Breakage in a Mixed Suspension Crystallizer," *Kristall Technik*, **8,** 931 (1973).

Gahn, C., and A. Mersmann, "The Brittleness of Substances Crystallized in Industrial Processes," *Powder Tech.*, **85,** 71 (1995).

Kelly, E. G., and D. J. Spottiswood, *Introduction to Mineral Processing*, Wiley, New York, pp. 113–123 (1982).

Mazzarotta, B., "Abrasion and Breakage Phenomena in Agitated Crystal Suspensions," *Chem. Eng. Sci.*, **47,** 12, 3105 (1992).

Mazzarotta, B., "Comminution Phenomena in Stirred Sugar Suspensions," *AIChE Symp. Ser.*, **89**(293), 112 (1993).

Nienow, A. W., and R. Conti, "Particle Abrasion at High Solids Concentration in Stirred Vessels," *Chem. Eng. Sci.*, **33,** 1077 (1978).

Rosenbrock, H. H., and C. Storey, *Computational Techniques for Chemical Engineers*, Pergamon Press, London (1966).

Stanley, G. G., "Mechanisms in the Autogenous Mill and Their Mathematical Representation," *J. S. Afr. Inst. Min. Metall.*, **75,** 77 (1974).

Strickland-Constable, R. F., *Kinetics and Mechanism of Crystallization*, Academic Press, London (1968).

Synowiec, P., A. G. Jones, and P. Ayazi-Shamlou, "Crystal Break-up in Dilute Turbulently Agitated Suspensions," *Chem. Eng. Sci.*, **48,** 3485 (1993).

Manuscript received Oct. 23, 1995, and revision received May 24, 1996.